Title

Total Synthesis of the Galbulimima Alkaloids Himandravine and GB17 Using Biomimetic Diels–Alder Reactions of Double Diene Precursors

Journal

Journal of the American Chemical Society, 137(34)

ISSN

0002-7863

Authors

Larson, Reed T
Pemberton, Ryan P
Franke, Jenna M
et al.

Publication Date

2015-09-02

DOI

10.1021/jacs.5b07710

Peer reviewed

HHS Public Access

Author manuscript

J Am Chem Soc. Author manuscript; available in PMC 2016 September 02.

Published in final edited form as:

J Am Chem Soc. 2015 September 2; 137(34): 11197–11204. doi:10.1021/jacs.5b07710.

Total Synthesis of the *Galbulimima* Alkaloids Himandravine and GB17 Using Biomimetic Diels–Alder Reactions of Double Diene Precursors

Reed T. Larson[†], **Ryan P. Pemberton**[‡], **Jenna M. Franke**[†], **Dean J. Tantillo**[‡,*], and **Regan J. Thomson**[†,*]

[†]Department of Chemistry, Northwestern University, 2145 Sheridan Road, Evanston, Illinois 60208, United States

[‡]Department of Chemistry, University of California—Davis, 1 Shields Avenue, Davis, California 95616, United States

Abstract

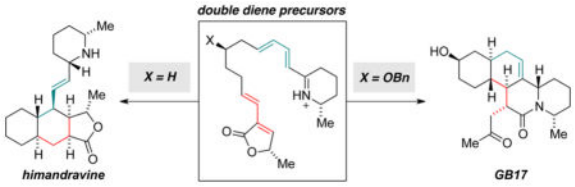

The enantioselective total syntheses of himandravine and GB17 were completed through a common biomimetic strategy involving Diels–Alder reactions of unusual double diene containing linear precursors. The double diene precursors, containing or lacking a C12 substituent as required to produce GB17 or himandravine, respectively, were found to undergo Diels–Alder reactions to afford mixtures of regioisomeric cycloadducts that map onto the alternative carbocyclic frameworks of both himandravine and GB17. Computational investigations revealed that these Diels–Alder reactions proceed via transition state structures of similar energy that have a high degree of bispericyclic character and that the low levels of regioselectivity observed in the reactions are a consequence of competing orbital interaction and distortion energies. The combined experimental and computational results provide valuable insights into the biosynthesis of the *Galbulimima* alkaloids.

[*]Corresponding Authors: djtantillo@ucdavis.edu, r-thomson@northwestern.edu.

Notes

The authors declare no competing financial interest.

Supporting Information

The Supporting Information is available free of charge on the ACS Publications website at DOI: 10.1021/jacs.5b07710.

X-ray data (CIF)

X-ray data (CIF)

X-ray data (CIF)

X-ray data (CIF)

All experimental procedures, computational data, and complete characterization (NMR, MS, IR, optical rotation) for all new compounds (PDF)

INTRODUCTION

The Diels–Alder reaction occupies a special position among organic reactions due to its ability to convert relatively simple starting materials into highly complex molecular frameworks in a single step.[1] Recognizing the reaction's potential, synthetic organic chemists have invested significant effort developing and applying a seemingly endless array of useful variations of the Diels–Alder reaction,[2] while simultaneously seeking to understand its fundamental theoretical basis.[3] The Diels–Alder reaction also occurs in Nature, with many natural products biosynthesized through pathways thought to involve the reaction.[4,5] Taking inspiration from these biosynthetic hypotheses, synthetic chemists have sought to replicate the proposed Diels–Alder reactions in the laboratory through so-called biomimetic syntheses.[4] Within this context, we were particularly drawn to the *Galbulimima* family of alkaloids (Figure 1). Isolated from *Galbulimima belgraveana* and *G. baccatta*, trees endemic to the rainforests of Northern Australia and Papua New Guinea, the *Galbulimima* alkaloids possess a range of unique polycyclic structures with decalin and piperidine rings serving to unify the family. During a period from 1956 to 1965, Taylor and co-workers reported the isolation of 28 alkaloids from *G. belgraveana* and *G. baccatta*, for which the structures of 22 were determined through a combination of spectroscopic analysis, structural degradation and interconversion, and semisynthesis.[6] In two papers published in 2009[7] and 2011,[8] Mander and co-workers reported the structures for five of the remaining six alkaloids, as well as two new family members. Based on structural similarities, the family has been divided into four classes (I–IV). Differences within a given class typically arise due to the extent of oxygenation about the carbocyclic skeleton. The Class IV alkaloids have little resemblance to other classes or to each other, and for this reason are sometimes known as "Miscellaneous" alkaloids.

Due to their fascinating structural features, the alkaloids have been popular targets for total synthesis.[9,10] Early work focused on the synthesis of himbacine (**1**), the simplest member of the family, with the first synthesis of **1** reported by Hart and Kozikowski in 1995.[11] Subsequent completed efforts were reported by the groups of both Chackalamannil[12] and Baldwin,[13,14] while the Terashima,[15] De Clercq,[16] and Sherburn[17] laboratories reported formal syntheses. Much of the excitement surrounding himbacine (**1**) was due to its reported activity as a potent and selective muscarinic receptor agonist (M2 receptor subtype K_i = 5–10 nM vs M3 subtype K_i = 150 nM).[18,19] Indeed, interest in himbacine as a potential therapeutic fueled a significant medicinal chemistry effort at Schering-Plough.[20] In the early 2000s, interest in the more complex members of the *Galbulimima* alkaloids was renewed following Mander and MacLachlan's inaugural synthesis of the Class III alkaloid GB13 (**5**) in 2003,[21] with ensuing total syntheses of GB13 (**5**) from the laboratories of Movassaghi,[22] Chackalamannil,[23] Evans,[24] Sarpong,[25] and Ma.[26] The chemical conversion of GB13 (**5**) into himgaline (**6**) was reported by both Chackalamannil[23] and Evans.[24] Movassaghi and coworkers reported an elegant synthesis of himandrine (**3**) in 2009 that remains the only Class II alkaloid to succumb to synthesis.[27] Of the Class IV alkaloids, GB16 (**7**) was synthesized by Ma and co-workers in 2010,[26] while our own group completed the synthesis of GB17 (**8**) in 2011.[28]

There has also been a great deal of speculation and interest regarding the biogenesis of the *Galbulimima* alkaloids (Figure 2). In 1961, Taylor and co-workers proposed that the Class I *Galbulimima* alkaloids were derived from nine acetate units, one pyruvate unit, and a molecule of ammonia to afford a linear precursor akin to **9**.[29] They subsequently expanded their proposal to include the formation of the Class II and III alkaloids from the same biogenetic precursor but were never specific regarding possible reaction details.[30] In 2005, Baldwin and co-workers refined the Taylor proposal by speculating that double diene **10** might undergo an intramolecular Diels–Alder reaction via iminium ion **12** to afford decalin **13**, which after reduction clearly maps onto the Class I alkaloids, such as himbacine (**1**) and himandravine (**2**).[13] Additional ideas about how species similar to decalin **13** might be transformed into the Class II and III alkaloids have been put forward by Baldwin,[31] Movassaghi,[22] and Mander.[8] Thus, the Diels–Alder reaction where the iminium ion conjugated diene (green) serves as the dienophile and the butenolide component (red) as the diene provides a unified route for the biogenesis of all Class I–III alkaloids, as well as GB16 (**7**)—a Class IV alkaloid,[7] but which could well be considered a member of Class II. The structure of GB17 (**8**), on the other hand, cannot be reconciled with this same Diels–Alder reaction. In their 2009 paper describing the structural elucidation of GB17 (**8**),[7] Mander and co-workers deduced that GB17 (**8**) must be derived from the alternative combination of dienes within a similar linear precursor (i.e., **11**). Thus, the Diels–Alder reaction of intermediate **14** where the iminium ion conjugated diene (green) serves as the diene and the butenolide component (red) as the dienophile leads to decalin **15**, which has the correct connectivity to produce GB17 (**8**).

The presence of two distinct dienes within a common linear precursor that can each potentially react as either the diene or the dienophile in an intramolecular Diels–Alder reaction to generate vastly different carbocyclic products is unusual. The placement of the single hydroxyl group within GB17 (**8**) drew our attention and led us to consider the nature of the possible regioisomeric Diels–Alder reaction transition state structures leading to the divergent product outcomes (i.e., **13** vs **15**). When X = OH, the proposed chairlike transition state of **12** would necessarily place the C12 hydroxyl group in an unfavorable axial orientation, while the alternative transition state leading to adduct **15** allows the hydroxyl group to occupy a more favorable equatorial orientation. Similar conformational Differences were utilized in Johnson's elegant synthesis of 11α-hydroxyprogesterone, wherein a single hydroxyl stereocenter dictated the stereochemical course of a biomimetic polyene cyclization.[32] We wondered whether this difference in conformational arrangement would be enough to favor the GB17 cycloadduct **15** over the corresponding Class I adduct **13**. We noted that no Class I alkaloids had been isolated that possess a C12 hydroxyl group, which led us to speculate that this pathway might be favored for the parent double diene lacking the hydroxyl group (i.e., **10**). Furthermore, Baldwin and co-workers reported only observing Class I adducts in their biomimetic synthesis;[13,14] they made no mention of the alternative Diels–Alder cycloadducts being formed, although at that time the structure of GB17 (**8**) had not been reported.

Consideration of the above information, coupled to our previous interest in both iminium ion Diels–Alder reactions[33] and the *Galbulimima* alkaloids,[28] led us to initiate research with the

goal to provide insight into these processes and investigate the nature of these proposed regiodivergent Diels–Alder reactions. Herein we report the synthesis of linear precursors both with and without hydroxyl groups, examine their capacity to participate in the proposed biomimetic Diels–Alder reactions, provide computational insights into these reactions, and report concise biomimetic syntheses of both himandravine (**2**) and GB17 (**8**).

RESULTS AND DISCUSSION

A common strategy to access both the hydroxylated and nonhydroxylated linear precursors required for the proposed biomimetic Diels–Alder reactions is outlined in Scheme 1. For the GB17 series (**A**), the requisite hydroxyl stereocenter was introduced with the necessary absolute configuration through an enantioselective Keck allylation[34] of aldehyde **16**,[35] thus providing ether **18** in 77% yield and 99% ee after benzylation. Allylic alcohol **19** was then generated over three standard steps in 91% yield. Removal of the silyl protecting group within **19** allowed for selective oxidation of the allylic alcohol using MnO_2 to afford an aldehyde, which was converted to the dimethyl acetal **20** (60% yield over three steps). Oxidation of the free primary alcohol within **20** followed by a Still–Gennari olefination[36] using phosphonate **A** generated cis-enoate **21** in 82% yield as a 3:1 mixture of *Z*:*E* isomers. Formation of the cis-enoate was crucial in order to obtain high trans-selectivity in the subsequent aldol reaction with aldehyde **B**.[37] Minimization of allylic strain within **21** during deprotonation with LDA enforces generation of the trans-configured double bond during formation of the extended enolate.[38] Diene **26** was thus produced with excellent trans-selectivity after lactonization and elimination, which avoided a problematic isomerization of the cis-diene that was formed in significant quantities if the trans-isomer of **21** was used in the aldol reaction with **B**.[11] Construction of the desired Diels–Alder reaction precursor (i.e., **28**) was then completed in 81% yield by cleavage of the dimethyl acetal within **26** and a subsequent Horner–Wadsworth–Emmons olefination using phosphonate **C**.[13] Synthesis of the corresponding precursor for the himandravine series (**B**) combines elements of our synthesis of the GB17 analogue (i.e, **28**) with the previously reported syntheses of himbacine (**1**).[11,13] Ultimately, the requisite linear precursor **29** could be obtained in good overall yield after 11 steps from cycloheptene (**22**).

In 2005, Baldwin and co-workers reported that exposure of double diene **29** to TFA (first at 0 °C, then at room temperature for 60 min) followed by the addition of sodium cyanoborohydride led to the formation of cycloadduct **39**, along with an equal quantity of the corresponding epimeric *trans*-piperidine isomer (from a nonselective reduction of the corresponding cyclic iminium ion).[13,14] They reported the conversion of these two cycloadducts to the corresponding natural products, himbacine (**1**) and himandravine (**2** via **39**). Given this report, we were highly surprised to find that exposure of OBn derivative **28** to TFA provided quantitative cleavage of the Boc group and formation of iminium ion **30**, but no sign of any products from cycloaddition (Scheme 2). In fact, iminium ion **30** proved quite stable at room temperature, allowing for its full structural characterization (^{1}and ^{13}C NMR, MS, and IR; see Supporting Information). Unfortunately, heating of **30** in refluxing chloroform failed to induce any reaction, while higher temperatures (benzene at reflux) led to decomposition. We therefore turned our attention to the corresponding investigation of

the himandravine series using double diene **29**, assuming that the OBn group within compound **28** was perturbing the system somehow. We hoped to replicate the Baldwin group's experiments but more thoroughly analyze the product outcomes in search of possible GB17-type isomers. Unfortunately, exposure of double diene **29** to the identical set of conditions reported by Baldwin and co-workers for this substrate gave rise only to iminium ion **31** and no cycloadducts.[14] Like the OBn derivative **30**, iminium ion **31** was also stable enough at room temperature to allow full characterization.

Frustrated by these outcomes, we were, however, inspired by a report from the Evans lab that demonstrated significant Differences in reactivity based on counterion identity for a series of related iminium ion Diels–Alder reactions.[39] We found that exposure of the TFA salts **30** or **31** to 1 equiv of methanesulfonic acid at 55 °C induced counterion metathesis and efficient intramolecular cycloaddition. Monitoring the reactions by 1H NMR spectroscopy over 5 days allowed us to observe the formation of himandravine-type cycloadducts **32** or **33**, along with GB17-type cycloadducts **34** or **35** that underwent complete isomerization to the conjugated iminium ions **36** or **37** in situ. The reaction mixtures were subsequently treated with sodium cyanoborohydride to yield the corresponding piperidine products. Reduction of the intermediate iminium ions gave rise to only a single *cis*-piperidine isomer for each case (i.e., where X = OBn or H), the result of selective axial delivery of hydride. The high selectivity of these reductions was somewhat surprising given that Baldwin and co-workers had reported obtaining a 1:1 mixture of piperidine epimers (see above).[14] Our experimental results are, however, consistent with reports of related reductions where high selectivity for axial delivery is also found.[40] Purification of the immediate mixtures following reduction proved challenging but was aided by selective Boc-protection of the himandravine-type adducts (**38a** or **39a**) allowing for their easy isolation from the corresponding GB17-type adducts. The GB17-type adducts **41** and **43** derived from linear precursor **29** could be separated using silica gel flash chromatography, while the corresponding GB17-type products derived from **28** could not be separated under a variety of conditions, including preparative HPLC. Pure samples of each compound were, however, readily obtained through an alternative route involving the thermal Diels–Alder reaction of ketone **28** (80 °C, 5 days), which led to separable cycloadducts that could be individually processed to **40** or **42** (see Supporting Information).

Stereochemical confirmation for **38a**, **40**, **41**, and **43** was established through single crystal X-ray crystallography (CCDC no. 1061572, 1061573, 1061574, and 1061575) as depicted in Scheme 2. The structure of cycloadduct **39a** was established by conversion to himandravine (**2**) by conjugate reduction of **39b** with Stryker's reagent and Boc-group cleavage thereby also completing the biomimetic synthesis of **2**. ^{1}H and ^{13}C NMR spectral data of himandravine (**2**) prepared in this manner matched those of an authentic sample, as well as published data.[41] Cycloadduct **42** could be transformed into GB17 (**8**) in two steps (Scheme 3). The first of these steps involved treatment of **42** with sodium methoxide, which induced a lactamization and redox isomerization event to form the diastereomeric ketones **44** and **45** in 85% yield. The major isomer **45** was converted to GB17 (**8**) following removal of the benzyl ether, thereby completing the biomimetic synthesis of GB17 (**8**) and simultaneously confirming the stereochemistry of cycloadduct **42**. ^{1}H and ^{13}C NMR spectral data of GB17

(**8**) prepared in this manner matched those of an authentic sample, as well as literature reports.[7,28]

Having established the identities of all cycloadducts, we could analyze the regiochemical and stereochemical outcome of the iminium ion Diels–Alder reactions of both linear precursors (i.e., **28** and **29**). For the GB17 series, the three cycloadducts **38a**, **40**, and **42** were formed in a 1:1:2 ratio, respectively, based upon analysis of the reaction mixture directly following reduction. Cycloadduct **42**, which possesses the correct connectivity and stereochemistry required for GB17 (**8**), was the slightly favored product. Formation of both **38a** and **40** forces the OBn substituent into an axial orientation. Apparently, the steric influence of the OBn group in determining the product distribution for this reaction is minimal and not the dominant control element we had hypothesized. This conclusion was reinforced by the Diels–Alder reaction outcomes of the himandravine series using double diene **29**, where an equal ratio of the three cycloadducts, **39a**, **41**, and **43**, was formed.

In order to gain insight into the nature of the regiodivergent Diels–Alder reactions involved in the synthesis of himandravine (**2**) and GB17 (**8**), we modeled the possible reactions of **31** (X = H) and its analogue with X = OH (a crude model of the OBn group in **30** and a model of a potential biosynthetic precursor to GB17). All structures (minima and transition state structures; counterions were not modeled) were optimized using the M06-2X functional[42] with the 6-311++G(2d,p) basis set[43,44] and the SMD continuum solvation model,[45] all with the Gaussian09 software package (see Supporting Information for additional details). The lack of selectivity observed experimentally for **30** and **31** is recapitulated in the computational results, which suggest that all three products—whether X = H or X = OR—form via transition state structures of similar free energy (Figure 3A).

Consistent with experimental observations, one type of transition state arrangement was preferred for himandravine formation (**TSA1** and **TSB1**), while both sets of possible endo GB17 arrangements were found to be competitive (**TSA2**/**B2** and **TSA3**/**B3**). For the himandravine case, facial selectivity is controlled by the methyl stereogenic center on the lactone leading to products **38a** and **39a** via **TSA1** and **TSB1**, respectively. For this scenario, the OR substituent has no influence on the reaction outcome. For the GB17 arrangement, the methyl substituent on the lactone is located far from the newly forming bonds and therefore exerts no influence on the facial selectivity (**TSB2** vs **TSB3**). Addition of the C12 hydroxyl substituent leads to a small preference for **TSA2** over **TSA3** (−0.6 kcal/mol), a result consistent with the 2:1 ratio of **40** and **42** observed experimentally. These computational and experimental values also align closely with reported A-values for the hydroxyl group and ether substituents.[46]

It is interesting that essentially no regioselectivity is observed in these cycloadditions, despite significant Differences in the structures of the dienes. Given that both dienes bear π-accepting groups, an inverse-electron demand mode is expected to predominate and the “matched” iminium-conjugated diene + lactone-conjugated dienophile pair might reasonably be expected to have a lower barrier than the “mismatched” ester-conjugated diene + α,β-unsaturated iminium-conjugated dienophile pair.

This expectation is consistent with frontier molecular orbital (FMO) energies for models **C** and **D** in Figures 3B and 3C—the HOMO–LUMO gap for the former pair (5.8 eV) is smaller than for the latter (7.8 eV). Why, then, do both reaction manifolds have very similar barriers? The answer is revealed by a distortion/interaction analysis (Figure 3C).[47–51] For the FMO-matched pair, which leads to the GB17 skeleton, the more reactive iminium-conjugated diene pays a higher distortion penalty in achieving its transition state geometry (~25 kcal/mol), due primarily to disruption of internal conjugation, than it does in the FMO-mismatched pair. Concomitantly, the lactone-conjugated dienophile pays a smaller distortion penalty. Overall, the total distortion penalties for the FMO-matched and FMO-mismatched pairs are approximately the same, but the distribution of distortion energies are different, with the greatest distortion penalty counteracting the inherent electrophilicity of the iminium-conjugated diene.

Notice also that the distances colored in red and green in each transition state structure are similar; bond formation along the red path would lead to the GB17 skeleton, whereas bond formation along the green path would lead to the himandravine skeleton (bond formation along the black path occurs during formation of both products). Related transition state geometries have been observed previously for other diene + diene Diels–Alder reactions that were bispericyclic—reactions where a single symmetrical (or pseudosymmetrical) transition state structure is connected to products of both possible diene–dienophile combinations via a post-transition state bifurcation on the potential energy surface.[52] Recently, Hoye and coworkers even described such a scenario for a biomimetic Diels–Alder reaction in the synthesis of the dimeric natural product, paracaseolide A.[53] Although we have not found solid evidence for a post-transition state bifurcation in our systems, perhaps due to their low symmetry, the associated secondary interactions between the dienes do appear to reduce the Differences in geometries and energies of our competing transition state structures.

Our results corroborate the biosynthetic hypothesis advanced by Baldwin and co-workers[13] that lactone-containing linear precursors participate in iminium ion Diels–Alder reactions to afford himandravine-type adducts, but we demonstrated that the alternative GB17-type adducts are also formed with poor selectivity between the two regioisomeric Diels–Alder reaction pathways. In the cases investigated, three out of the four possible endo Diels–Alder adducts were observed: both GB17-type diastereomers and one of the two possible himandravine-type stereoisomers. While our original hypothesis was that the presence of a C12 substituent in the linear Diels–Alder reaction precursor might allow the GB17-type adduct to be favored over the himandarive-type adduct, experimental results show that the C12 substituent exerts very little influence over the product distribution. It therefore seems most likely that the C12 hydroxyl group within GB17 (**8**) is introduced biosynthetically after a nonselective Diels–Alder reaction has occurred (see below). Late-stage hydroxylation is also consistent with the extensive degree of oxygenation that is observed in other members of the *Galbulimima* family, such as himandrine (**3**) and GB1 (**4**), for example.

Formation of the diastereomeric decalin ring system for the GB17 arrangement (i.e., **40**/**41**) is intriguing, and it is tempting to speculate that there may exist as yet identified alkaloids possessing this configuration. On the other hand, both decalin isomers derived from the himandravine arrangement are known in nature, yet only one isomer (i.e., **38**/**39**) was

observed in our experiments. Our results indicate that access to the diastereomeric decalin ring system required to generate the Class II, III and IV alkaloids (except GB17) would require a precursor with an epimeric methyl substituent on the lactone moiety. Alternative possibilities have been posited where the putative linear double diene precursor lacks this methyl stereocenter entirely, but these speculations have not yet been verified experimentally.[8,22,31] In such a situation, as depicted in Figure 4, it is reasonable to assume that both pairs of diastereomeric decalin systems would be produced from a single starting material such as **46**. In this unified scenario, **TS-47** would provide access to the Class II–IV alkaloids and GB17 via decalins **48** and **49**, respectively. The Class I alkaloids would then derive from decalin **51**, which forms via **TS-50**. If formed, the isomeric GB17-type adduct **52** would lead to currently unknown alkaloids.

CONCLUSIONS

Our combined experimental and computational studies have provided new insights into the factors governing the complex Diels–Alder reactions postulated to be involved in the biosynthesis of the *Galbulimima* alkaloids. Intermediate iminium ions underwent regiodivergent Diels–Alder reactions via transition state structures of similar energy to generate the carbocyclic skeletons of structurally distinct natural products, allowing for the biomimetic total synthesis of both himandravine (**2**) and GB17 (**8**). The orbital interactions associated with bispericyclic character appear to promote these Diels–Alder reactions and may play an important role in the formation of a variety of polycyclic natural products. It is intriguing to speculate that the structural diversity obtained from the putative double diene biosynthetic precursor for the *Galbulimima* alkaloids is Nature's version of "diversity oriented synthesis", where the production of multiple chemotypes from a single precursor might provide an evolutionary advantage to the producing organism. Further investigations into the biosynthetic machinery responsible for the formation of the putative double diene precursor, its regiodivergent Diels–Alder reactions, and subsequent transformations should further illuminate this remarkable family of natural products.

Supplementary Material

Refer to Web version on PubMed Central for supplementary material.

Acknowledgments

Support from the National Institutes of Health (R01GM085322) and U.S. National Science Foundation (CHE-030089 via XSEDE) is gratefully acknowledged. We thank Professor Lewis N. Mander (The Australian National University) for helpful discussions and authentic samples of GB17 and himandravine.

References

1. Diels O, Alder K. Justus Liebigs Ann Chem. 1928; 460:98.
2. Nicolaou KC, Snyder SA, Montagnon T, Vassilikogiannakis G. Angew Chem, Int Ed. 2002; 41:1668.
3. Houk KN, Gonzalez J, Li Y. Acc Chem Res. 1995; 28:81.
4. Stocking EM, Williams RM. Angew Chem, Int Ed. 2003; 42:3078.
5. Oikawa H, Tokiwano T. Nat Prod Rep. 2004; 21:321. [PubMed: 15162222]

6. Binns S, Dunstan P, Guise G, Holder G, Hollis A, McCredie R, Pinhey J, Prager R, Rasmussen M, Ritchie E, Taylor W. Aust J Chem. 1965; 18:569.
7. Mander LN, Willis AC, Herlt AJ, Taylor WC. Tetrahedron Lett. 2009; 50:7089.
8. Bradford TA, Willis AC, White JM, Herlt AJ, Taylor WC, Mander LN. Tetrahedron Lett. 2011; 52:188.
9. Rinner U, Lentsch C, Aichinger C. Synthesis. 2010; 2010:3763.
10. Bhattacharyya D. Tetrahedron. 2011; 67:5525.
11. Hart DJ, Wu WL, Kozikowski AP. J Am Chem Soc. 1995; 117:9369.
12. Chackalamannil S, Davies RJ, Asberom T, Doller D, Leone D. J Am Chem Soc. 1996; 118:9812.
13. Tchabanenko K, Adlington RM, Cowley AR, Baldwin JE. Org Lett. 2005; 7:585. [PubMed: 15704900]
14. The Baldwin lab's publication (ref 13) regarding the biomimetic synthesis of himbacine has recently been retracted. Tchabanenko K, Adlington RM, Cowley AR, Baldwin JE. Org Lett. 2015; 17:3190. [PubMed: 26087894]
15. Takadoi M, Katoh T, Ishiwata A, Terashima S. Tetrahedron Lett. 1999; 40:3399.
16. Gao LJ, Waelbroeck M, Hofman S, Van Haver D, Milanesio M, Viterbo D, De Clercq PJ. Bioorg Med Chem Lett. 2002; 12:1909. [PubMed: 12113806]
17. Wong LSM, Sherburn MS. Org Lett. 2003; 5:3603. [PubMed: 14507183]
18. Darroch S, Taylor W, Choo LK, Mitchelson F. Eur J Pharmacol. 1990; 183:1720.
19. Miller JH, Aagaard PJ, Gibson VA, McKinney M. J Pharmacol Exp Ther. 1992; 263:663. [PubMed: 1331410]
20. Chackalamannil S, Wang Y, Greenlee WJ, Hu Z, Xia Y, Ahn HS, Boykow G, Hsieh Y, Palamanda J, Agans-Fantuzzi J, Kurowski S, Graziano M, Chintala M. J Med Chem. 2008; 51:3061. [PubMed: 18447380]
21. Mander LN, McLachlan MM. J Am Chem Soc. 2003; 125:2400. [PubMed: 12603121]
22. Movassaghi M, Hunt DK, Tjandra M. J Am Chem Soc. 2006; 128:8126. [PubMed: 16787063]
23. Shah U, Chackalamannil S, Ganguly AK, Chelliah M, Kolotuchin S, Buevich A, McPhail A. J Am Chem Soc. 2006; 128:12654. [PubMed: 17002352]
24. Evans DA, Adams DJ. J Am Chem Soc. 2007; 129:1048. [PubMed: 17263383]
25. Larson KK, Sarpong R. J Am Chem Soc. 2009; 131:13244. [PubMed: 19754185]
26. Zi WW, Yu SY, Ma DW. Angew Chem, Int Ed. 2010; 49:5887.
27. Movassaghi M, Tjandra M, Qi J. J Am Chem Soc. 2009; 131:9648. [PubMed: 19555115]
28. Larson RT, Clift MD, Thomson RJ. Angew Chem, Int Ed. 2012; 51:2481.
29. Pinhey JT, Ritchie E, Taylor WC. Aust J Chem. 1961; 14:106.
30. Mander LN, Prager RH, Rasmussen M, Ritchie E, Taylor WC. Aust J Chem. 1967; 20:1705.
31. Tchabanenko K, Chesworth R, Parker JS, Anand NK, Russell AT, Adlington RM, Baldwin JE. Tetrahedron. 2005; 61:11649.
32. Johnson WS, Brinkmeyer RS, Kapoor VM, Yarnell TM. J Am Chem Soc. 1977; 99:8341. [PubMed: 925270]
33. Kim J, Thomson RJ. Angew Chem, Int Ed. 2007; 46:3104.
34. Keck GE, Tarbet KH, Geraci LS. J Am Chem Soc. 1993; 115:8467.
35. Frankowski KJ, Golden JE, Zeng Y, Lei Y, Aubé J. J Am Chem Soc. 2008; 130:6018. [PubMed: 18396881]
36. Still WC, Gennari C. Tetrahedron Lett. 1983; 24:4405.
37. Ito Y, Kobayashi Y, Kawabata T, Takase M, Terashima S. Tetrahedron. 1989; 45:5767.
38. Kende AS, Toder BH. J Org Chem. 1982; 47:163.
39. Marcoux D, Bindschädler P, Speed AWH, Chiu A, Pero JE, Borg GA, Evans DA. Org Lett. 2011; 13:3758. [PubMed: 21678927]
40. Ryckman DM, Stevens RV. J Org Chem. 1987; 52:4274.
41. Chackalamannil S, Davies R, McPhail AT. Org Lett. 2001; 3:1427. [PubMed: 11388833]
42. Zhao Y, Truhlar DG. Theor Chem Acc. 2008; 120:215.

43. McLean AD, Chandler GS. J Chem Phys. 1980; 72:5639.
44. Krishnan R, Binkley JS, Seeger R, Pople JA. J Chem Phys. 1980; 72:650.
45. Marenich AV, Cramer CJ, Truhlar DG. J Phys Chem B. 2009; 113:6378. [PubMed: 19366259]
46. Eliel, EL.; Wilen, SH.; Mander, LN. Stereochemistry of Organic Compounds. Wiley; New York: 1994.
47. Ess DH, Houk KN. J Am Chem Soc. 2007; 129:10646. [PubMed: 17685614]
48. Ess DH, Houk KN. J Am Chem Soc. 2008; 130:10187. [PubMed: 18613669]
49. Hayden AE, Houk KN. J Am Chem Soc. 2009; 131:4084. [PubMed: 19256544]
50. Lopez SA, Houk KN. J Org Chem. 2013; 78:1778. [PubMed: 22764840]
51. van Zeist WJ, Bickelhaupt FM. Org Biomol Chem. 2010; 8:3118. [PubMed: 20490400]
52. Ess DH, Wheeler SE, Iafe RG, Xu L, Çelebi-Ölçüm N, Houk KN. Angew Chem, Int Ed. 2008; 47:7592.
53. Wang T, Hoye TR. Nat Chem. 2015; 7:641. [PubMed: 26201740]

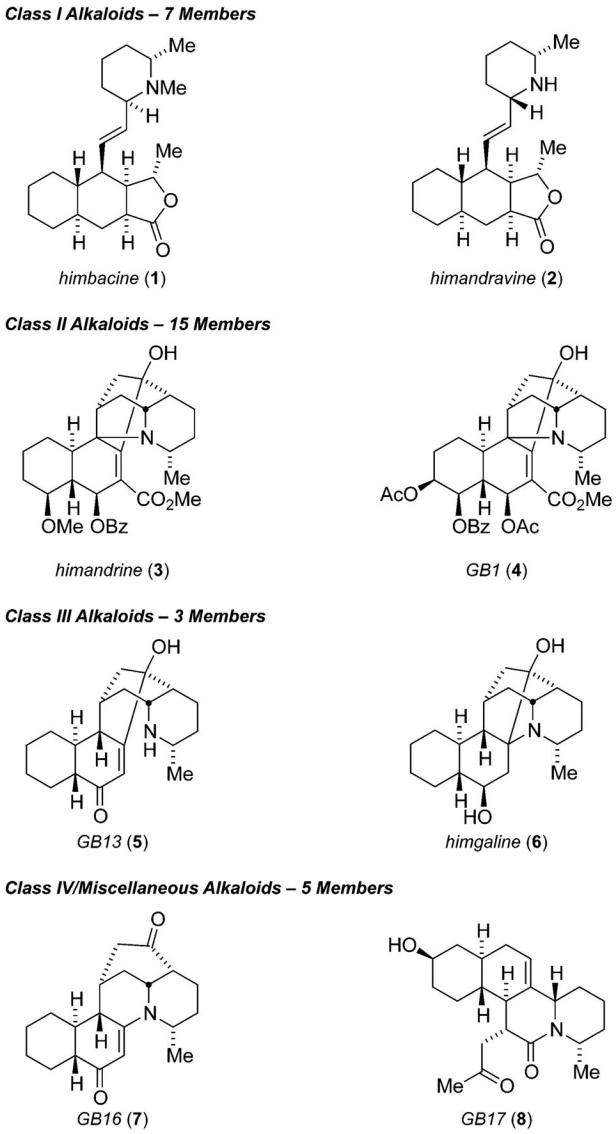

Figure 1.
Representative *Galbulimima* alkaloids.

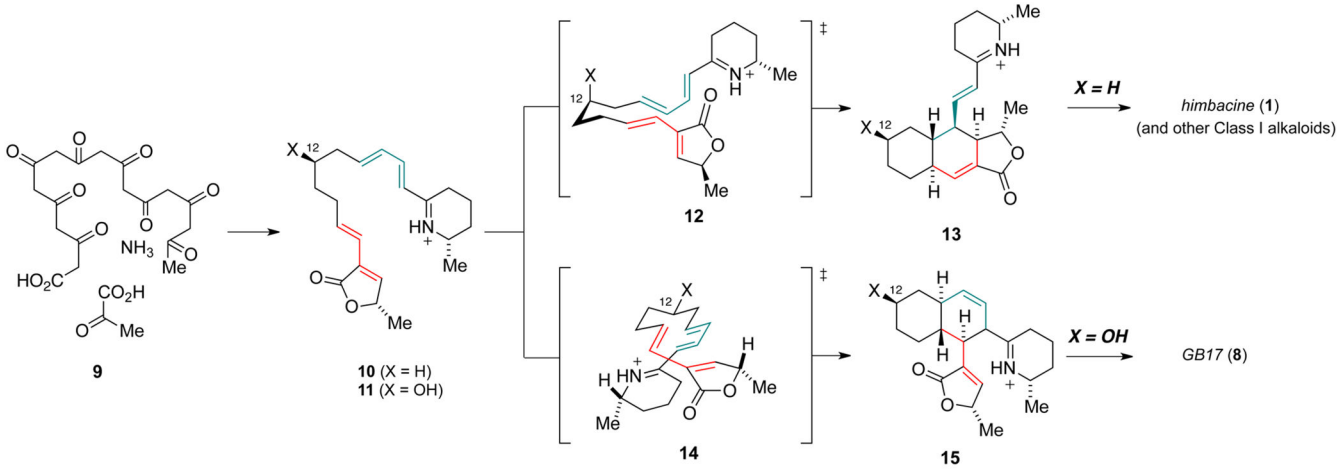

Figure 2.
Proposed regiodivergent [4 + 2] cycloadditions in *Galbulimima* alkaloid biosynthesis.

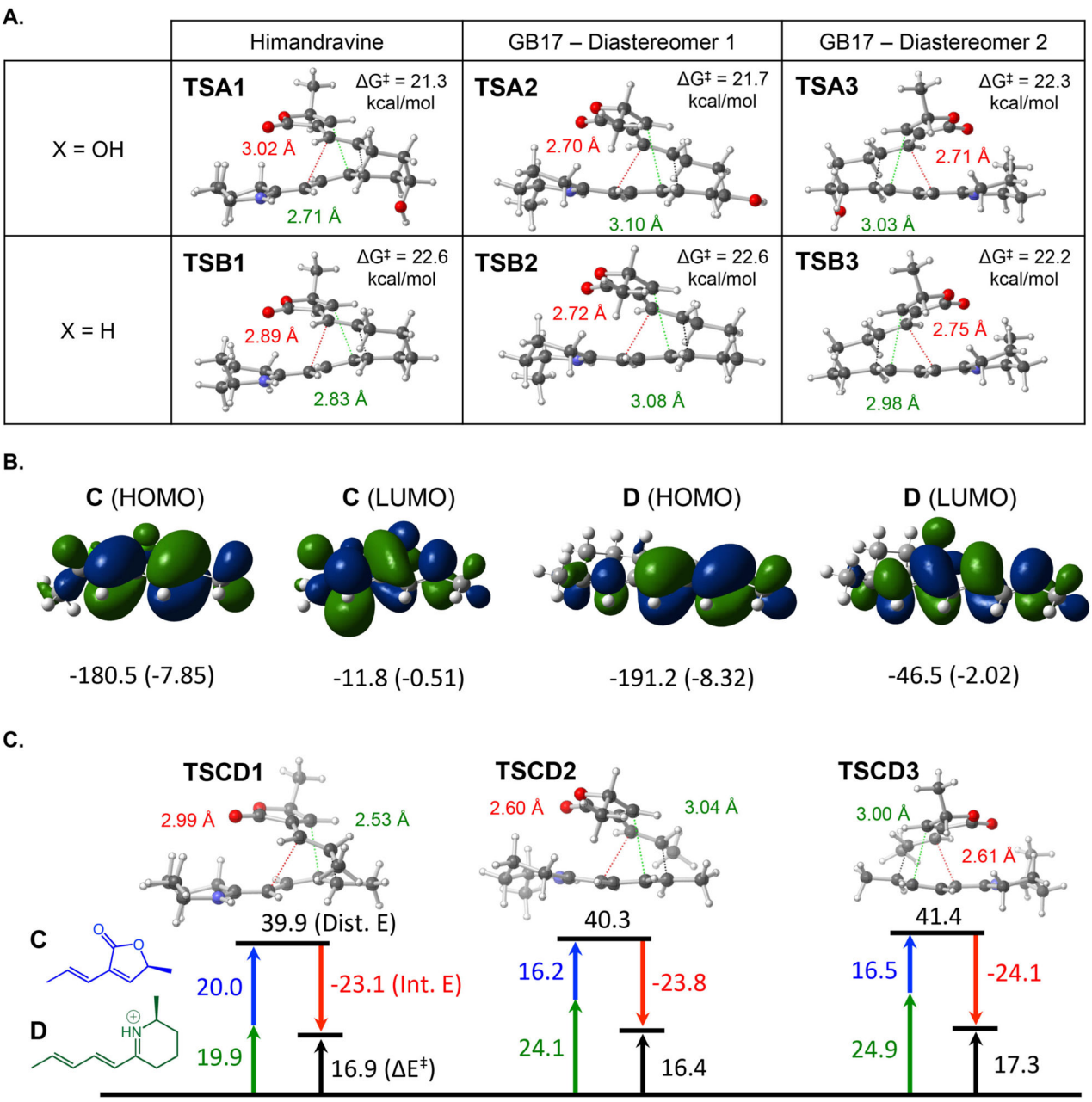

Figure 3.

(A) Diels–Alder reaction transition state structures. Free energy barriers (Δ*G*‡; kcal/mol) are relative to reactant structures. A complete conformational search was performed on the X = OH reactant, and the best conformer used to calculate both the X = OH and X = H barrier heights. C–C distances are shown in Å. (B) Highest occupied and lowest unoccupied molecular orbitals of **C** and **D**. Orbital energies are shown in kcal/mol (plain text) and eV (parentheses). (C) Distortion/interaction energy analysis for Diels–Alder reactions of **C** + **D**. All energies shown (kcal/mol) are electronic (zero-point energy uncorrected). Individual distortion energies for **C** and **D** are shown to the left of the blue and green arrows, respectively, and the sum of those is also given above the top black line. Calculated barriers

(Δ*E*‡) are shown to the right of the black arrow, and interaction energies (Int. *E*) are shown to the right of the red arrow; the latter are calculated as the difference between the total distortion energy and Δ*E*‡.

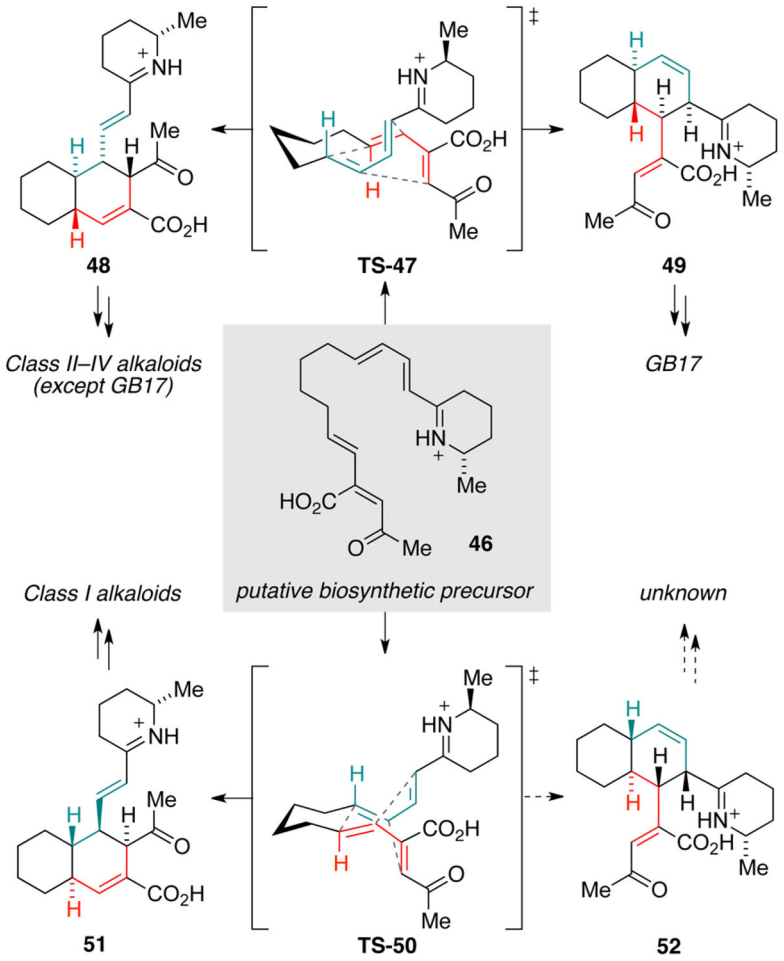

Figure 4.

Further speculation for the biosynthesis of the *Galbulimima* alkaloids. Double diene **46** serves as a common intermediate leading to all known family members by way of the bispericyclictype transition state structures, **TS-47** and **TS-50**. Additional tailoring of the initial cycloadducts **48**, **49**, and **51** by way of bond-forming reactions, rearrangements, and/or oxidations/reductions would give rise to all of the currently known *Galbulimima* alkaloids.

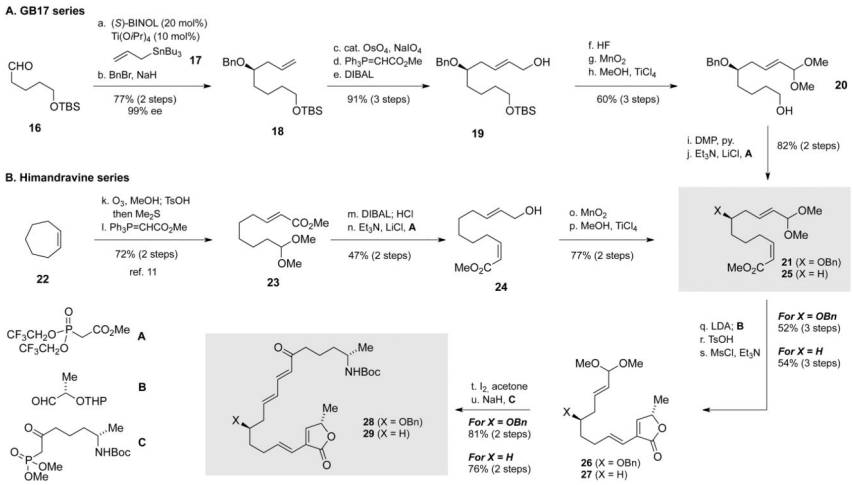

Scheme 1[a]

[a]Reagents and conditions: a. Twenty mol % (*S*)-BINOL, 10 mol % Ti(O*i*Pr)$_4$, 4 Å molecular sieves, allyltributylstannane, 78%; b. BnBr, NaH, Bu_4NI, 99% ee, 99%; c. Two mol % OsO_4, 2,6-lutidine, $NaIO_4$, 1,4-dioxanes:water, 96%; d. methyl (triphenylphosphoranylidene)acetate, THF, reflux, 96%; e. DIBAL, −78 °C → 0 °C, 99%; f. 40–45% aq. HF, 0 °C, 99%; g. MnO_2, 76%; h. 1.0 M $TiCl_4$, MeOH, Et_3N, 94%; i. Dess–Martin periodinane, pyridine, 86%; j. **A**, Et_3N, LiCl, 3:1 *Z:E*, 95%; k. O_3, MeOH:TsOH; Me_2S; l. methyl (triphenylphosphoranylidene)acetate, 72% (over 2 steps from **22**); m. DIBAL, −78 °C → 0 °C; 1.0 M HCl, acetone; n. **A**, Et_3N, LiCl, 47% (over 3 steps from **23**); o. MnO_2, 83%; p. 1.0 M $TiCl_4$, MeOH, Et_3N, 93%; q. LDA; then **B**; r. TsOH·H_2O MeOH; s. Et_3N, MsCl, 52% (**26** over 3 steps from **21**) or 54% (**27** over 3 steps from **25**); t. I_2, acetone; u. **C**, NaH, 0 °C → rt, **28** (81% over 2 steps from **26**) or **29** (76% over 2 steps from **27**).

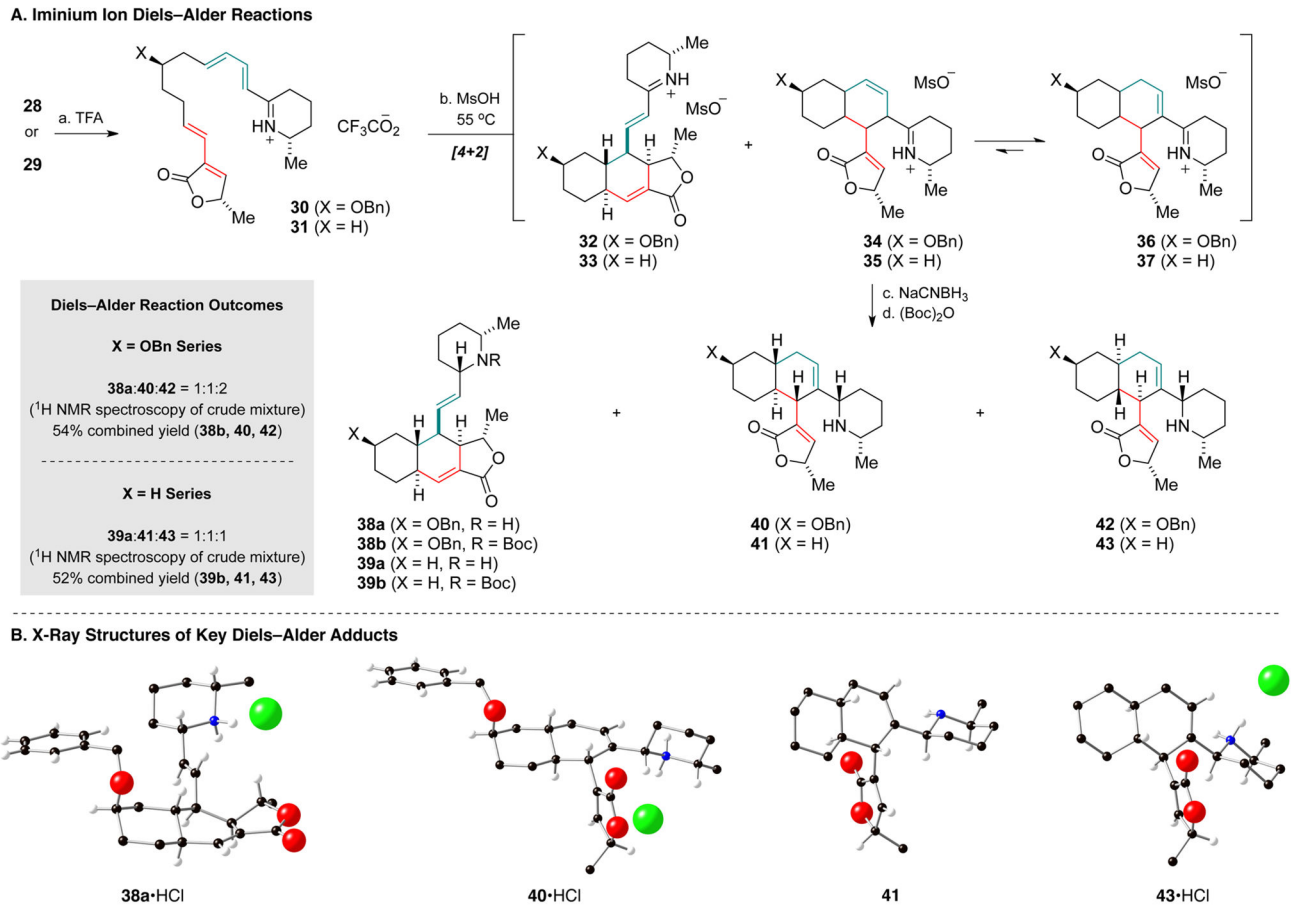

Scheme 2[a]

[a]Reagents and conditions: a. TFA, DCM 0 °C → rt; b. MsOH, $CDCl_3$, 55 °C, 5–7 days; c. $NaCNBH_3$, EtOH, 0 °C → rt, 1:1:2 ratio of **38a:40:42** (from **28**) or 1:1:1 ratio of **39a:41:43** (from **29**) as determined by 1H NMR spectroscopy of unpurified reaction mixture; d. $(Boc)_2O$, Et_3N, **38b** (15%) + **40** and **42** (39% of mixture) from **28** or **39b** (22%), **41** (18%) + **43** (12%) from **29**.

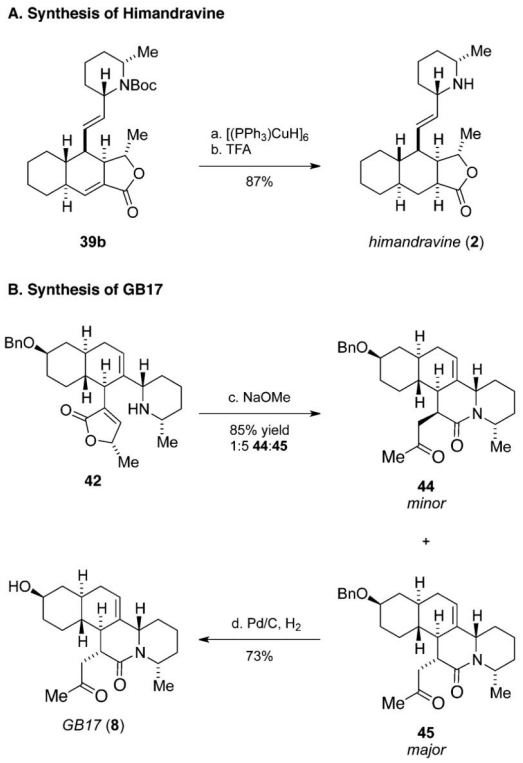

Scheme 3[a]

[a]Reagents and conditions: a. $PhSiH_3$, $[(PPh_3)CuH]_6$, 99%; b. TFA, DCM 0 °C → rt, 87%; c. NaOMe, MeOH, 2 days, **44** (15%) + **45** (70%); d. 10% Pd/C, H_2, EtOH, 73%.